MRI Denoising using Visual System Response Model Simulating PCNN

Sudeb Das*
Machine Intelligence Unit
Indian Statistical Institute
203 B. T. Road, Kolkata-108, India
to.sudeb@gmail.com

Malay Kumar Kundu
Machine Intelligence Unit
Indian Statistical Institute
203 B. T. Road, Kolkata-108, India
malay@isical.ac.in

ABSTRACT

A novel improved Non-local Means (NLM) filtering scheme for MR images is proposed based on a simplified pulse-coupled neural network (PCNN) which follows mammal's visual/perceptual response characteristics. The proposed scheme is a two-stage filtering technique. In the first stage, the noisy MR image is passed through a PCNN and the firing time output (time signature) of the PCNN is recorded. The time signature is used to pre-select a subset of pixels in non-local vicinities, depending on their similarities with the pixel of interest. In the second stage, improved unbiased NLM (IUNLM) is applied to denoise the pixel of interest only considering the contributions of the pre-selected subset of pixels in the non-local vicinities. Extensive experiments and comparisons with state-of-the-art MRI denoising techniques were carried out to evaluate the performance of the proposed scheme. The results suggest supporting evidence of the effectiveness of the proposed scheme in MR image denoising.

Categories and Subject Descriptors

I.4.3 [**Image Processing and Computer Vision**]: Enhancement; I.2 [**Artificial Intelligence**]: Applications and Expert Systems; I.5.4 [**Pattern Recognition**]: Applications

Keywords

Magnetic resonance, image enhancement, non-local means, pulse coupled neural network

*At present, S. Das is with Tata Consultancy Services, Innovation Lab, Building 1B, Ecospace, Plot - IIF/12, New Town, Rajarhat, Kolkata-700156, WB, India, http://www.tcs.com.

PerMIn '15, February 26-27, 2015, Kolkata, West Bengal, India

http://dx.doi.org/10.1145/2708463.2709031.

1. INTRODUCTION

As a low-risk, fast, non-invasive imaging technique, MRI provides high quality and high contrast images of anatomical structures and functional activities of different organs [26]. Over the years MRI technology has advanced significantly to be more cost-effective providing improved spatio-temporal resolution as well as reducing the acquisition time. However, the quest of any of these objectives results in images with low signal-to-noise ratio (SNR) and exhibits significant artifacts (e.g, noise, partial voluming, and bias field etc.), which are undesirable. These artifacts limit the accuracy of computer-aided diagnosis, clinical visual inspection and the performance of subsequent high level post-processing procedures e.g., segmentation, registration, tracking etc. Therefore, pre/post-acquisition enhancement steps are essential for reducing these artifacts in MR images [26, 19].

Over the years, many approaches have been proposed to address the difficult problem of MR image denoising. Generally, these existing schemes can be grouped into three different categories. The first group of approaches belongs to variational methods and are based on the numerical solution of certain partial differential equations (PDEs) [11, 15]. The second category of MRI denoising techniques is based on the sparseness property of certain linear transforms [20, 21]. Finally, the nonlocal means (NLM) filtering techniques encompass the approaches of the third category. Originally proposed by Buades et al. [3], NLM is a very simple and effective way to reduce noise while minimally affecting the intrinsic original structures of the image. Several modifications of the original NLM algorithm have been proposed by various researchers for denoising MR images [6, 23, 5, 10, 13, 17, 18]. A good review of several other variations of NLM filter for MR image denoising is given in [19].

The main drawback of the existing MRI denoising schemes based on NLM filter is the need for very intensive computations due to the reckoning of the squared distance between the compared pixels. Our main objective in this article is to propose an efficient way of reducing NLM filter's computational burden and at the same time achieving better denoised MR images. In this regard, our main contribution is the use of image's time signature information obtained by applying a simplified pulse coupled neural network (PCNN) on the MR image, to pre-select significant pixels in the search window of NLM. In the proposed technique this pre-selection helps in finding the significant pixels only for

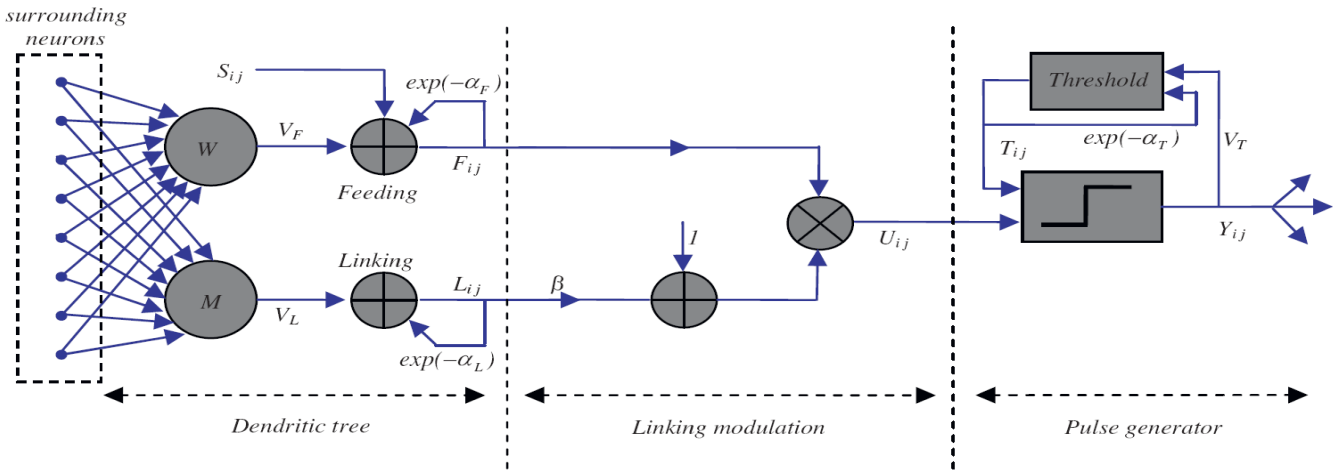

Figure 1: Structure of PCNN.

which the squared distances are calculated in the subsequent phase of the method. As a result of this pre-selection not only the computational burden of NLM filter reduces, but also we achieve better denoised MR images.

The rest of the paper is organized as follows. In Section 2, we briefly describe the NLM denoising technique and the PCNN. We outline in Section 3 the proposed PCNN adaptive unbiased NLM technique. Experimental results and comparisons are presented in Section 4, and we draw conclusion in Section 5.

2. MATERIALS

In this section we first briefly describe the NLM filtering technique in MR image denoising. Then, we discuss the PCNN mechanism and how it is used for image denoising purpose.

2.1 Non-local Means

In the standard formulation of NLM, given an image X, the filtered value $NLM(X(p))$ at a (noisy) pixel p with intensity value $X(p)$ is calculated as [3]:

$$NLM(X(p)) = \sum_{\forall q \in \Omega} w(p,q)X(q), \tag{1}$$

where, Ω is a large '*search window*' centered at pixel p (in [3] Ω is considered to be the entire image i.e., $\Omega = X$) and $w(p,q)$ is the weight assigned to pixel q with respect to pixel p, according to the similarity between two patches N_p and N_q centered at p and q, respectively, and is calculated:

$$w(p,q) = \frac{1}{Z(p)} e^{-\frac{d(p,q)}{h^2}}, \tag{2}$$

$$Z(p) = \sum_{q \in \Omega} e^{-\frac{d(p,q)}{h^2}}, \tag{3}$$

where, $Z(p)$ is a normalizing constant: $\sum_q w(p,q) = 1$, and $0 \leq w(p,q) \leq 1$. The parameter h is an exponential decay control parameter and d is the Gaussian weighted Euclidean distance of all the pixels of each neighborhood:

$$d(p,q) = G_p ||X(N_p) - X(N_q)||^2_{R_{sim}}, \tag{4}$$

where, G_p is a normalized Gaussian weighting function with zero mean and σ standard deviation (usually set to 1). The $X(N_p)$ is defined as a square '*neighborhood window*' centered around pixel p with a user-defined radius R_{sim}. When $p = q$, the self similarity is very high and thus can produce an over-weighting effect in Eq. 1. To solve this problem, $w(p,p)$ is calculated as:

$$w(p,p) = max(w(p,q) \forall q \neq p), \tag{5}$$

In [17], Manjon et al. have proposed a Rician-adapted version of the NLM filter for MR images, overcoming the problem of signal dependant noise bias of MRI. Their scheme, called the unbiased NLM (UNLM) follows the idea of [20], that in the squared magnitude MR image, the noise bias ($2\sigma^2$) is no longer signal-dependant and can be easily removed:

$$UNLM(X) = \sqrt{NLM(X)^2 - 2\sigma^2}, \tag{6}$$

The NLM filter outperforms state-of-the-art denoising techniques such as total variation (TV) minimization, anisotropy diffusion (AD) or translation invariant wavelet thresholding etc. Nevertheless, the main shortcoming of the NLM filter is the computational burden due its complexity. Moreover, considering all the pixels' contributions for denoising a particular pixel– often causes negative impact in the denoising process.

2.2 Pulse-Coupled Neural Network

PCNN simulates the processing mechanism of mammal's visual cortex and characterized by global coupling and pulse synchronization of neurons [9, 25]. It is a single layered, two-dimensional, laterally connected neural network of pulse coupled neurons. The PCNN neuron's structure is shown in Fig. 1. The neuron consists of an input part (dendritic tree), linking part and a pulse generator. PCNN is an excellent tool for image processing [25, 7, 8]. Considering the applications of MRI denoising, and in order to improve the computational efficiency, we use a simplified PCNN model:

$$F_{i,j}[n] = S_{i,j}, \tag{7}$$

$$L_{i,j}[n] = L_{i,j}[n-1] + \sum_{k,l} w_{i,j,k,l} Y_{i,j}[n-1], \tag{8}$$

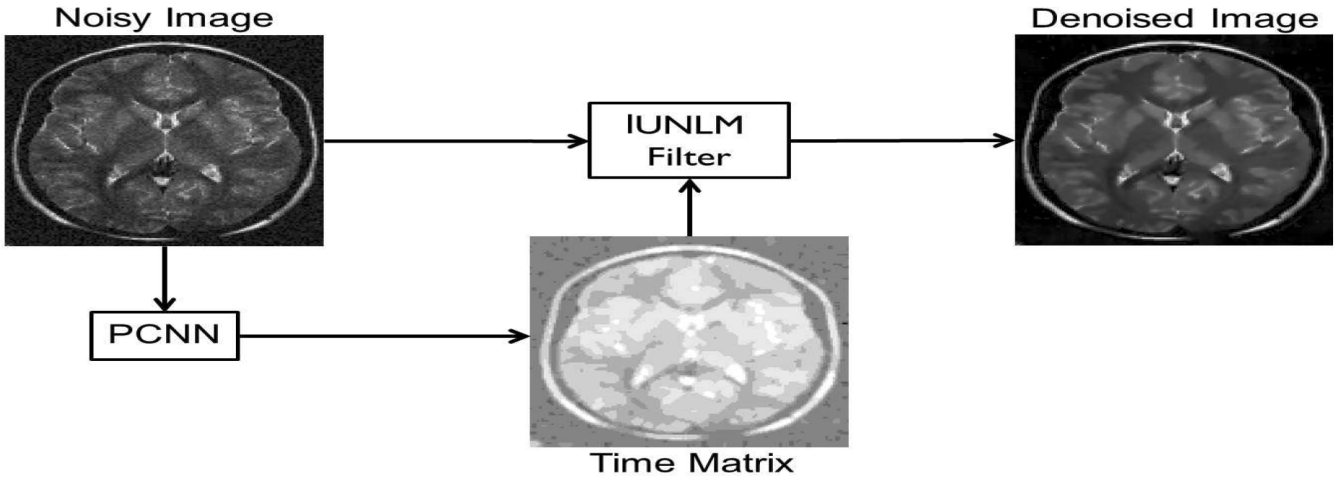

Figure 2: Block diagram of the proposed scheme.

$$U_{i,j}[n] = F_{i,j}[n](1 + \beta L_{i,j}[n]), \tag{9}$$

$$Y_{i,j}[n] = \begin{cases} 1, & U_{i,j}[n] > T_{i,j}[n-1], \\ 0, & \text{otherwise}, \end{cases} \tag{10}$$

$$T_{i,j}[n] = T_{i,j}[n-1] + V_T Y_{i,j}[n] \tag{11}$$

where the indexes i and j refer to the pixel location in the image, k and l refer to the dislocation in a symmetric neighborhood around one pixel, and n denotes the current iteration (discrete time step). Here n varies from 1 to N (total number of iterations). The two main components F and L are called feeding and linking, respectively. $w_{i,j,k,l}$ is the synaptic weight coefficient and S is the external stimulus (in the proposed scheme it is the averaged intensity value considering a window surrounding the pixel of interest). The linking modulation is given in Eq.(9), where $U_{i,j}[n]$ is the internal state of the neuron and β is the linking parameter. The pulse generator determines the firing events in the model in Eq.(10). $Y_{i,j}[n]$ depends on the internal state and threshold. The dynamic threshold of the neuron is Eq.(11), where V_T is the normalized constant. The firing time output (time matrix) is computed as follows:

$$G(i,j) = \sum_{n=1}^{N} Y_{i,j}[n], \tag{12}$$

The time matrix, generated by PCNN, contains useful information related to spatial structure of the image under processing. It is a mapping from image spatial information to time sequence.

3. PCNN ADAPTIVE NLM

According to the working principle of PCNN, if a neuron is activated at some iteration, at the next iteration those pixels having approximate intensity around it will be activated too. Whereas, if the gray value of a pixel has apparent difference with those of the pixels around it, the neuron corresponding to the pixel will be activated before or after the neurons around it. As we know, except for the geometric structural details (edges, corners, contours etc.) most of the local areas of an image have high correlation. Therefore, if a neuron cannot fires synchronously with others around it, it can he thought that the gray value of the pixel has been degraded by noise, and proper subsequent algorithms should be taken to restore it [27, 14, 16, 4, 28, 12].

Based upon the above mentioned properties of PCNN, in this article we have proposed an alternative way of pixel pre-selection for NLM filter. The proposed alteration is based upon the improved version (pixel pre-selection through local mean) of the UNLM proposed in [17]. The block diagram of the proposed PCNN adaptive improved unbiased NLM (PCNN-AIUNLM) scheme is shown in Fig. 2. The salient steps of the proposed scheme are as follows:

1. Estimate the noise of the image (noise estimation is described later).

2. Input the normalized and local averaged (considering a window) pixels' values of the noisy MR image (X) to motivate the neurons of the used PCNN and generate pulse of neurons using Eqs. 7–11.

3. Record the PCNN's output (time matrix) information G using Eq. 12.

4. For every pixel $X(p)$ in the image X use Eq. 1 to compute the filtered value following the conditions:

$$w(p,q) = \begin{cases} \frac{1}{Z(p)} e^{-\frac{d(p,q)}{h^2}}, & \text{if } Cond_1 \text{ or } Cond_2 \\ 0, & \text{otherwise} \end{cases} \tag{13}$$

   where $Cond_1 : |G(p) - G(q)| \leq t$, t represents a denoising parameter. It controls the tradeoff between the denoising performance and computational cost. In general, increasing the value of t will improve the result but with higher time requirement and vice versa. $Cond_2 : |Mean(X(N_p)) - Mean(X(N_q))| < \sigma$. The parameter σ denotes the standard deviation of the noise.

5. For every pixel in the image calculate the unbiased value by applying Eq. 6.

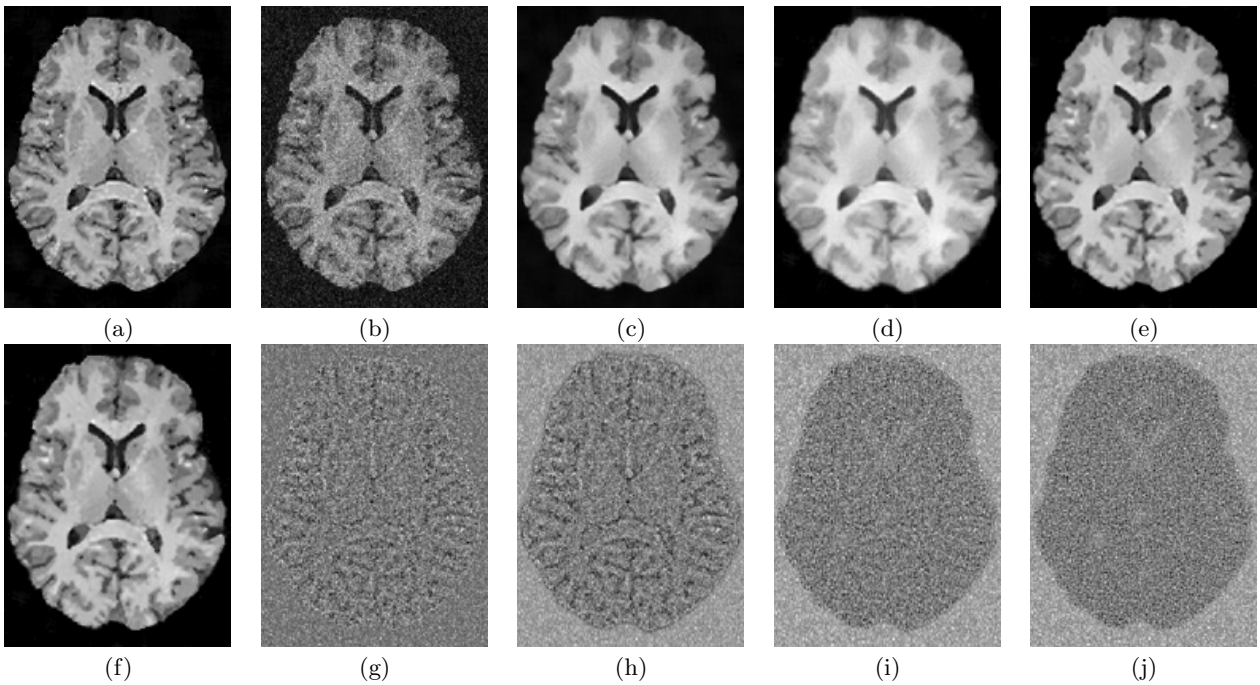

Figure 3: Synthetic MR image: (a) Noise-free image, (b) noisy image (Rician noise level = 10%), (c) NLM-output [2], (d) UNLM-output [17], (e) IUNLM-output, (f) PCNN-AIUNLM output, (g) residual of NLM, (h) residual of UNLM, (i) residual of IUNLM and (j) residual of PCNN-AIUNLM.

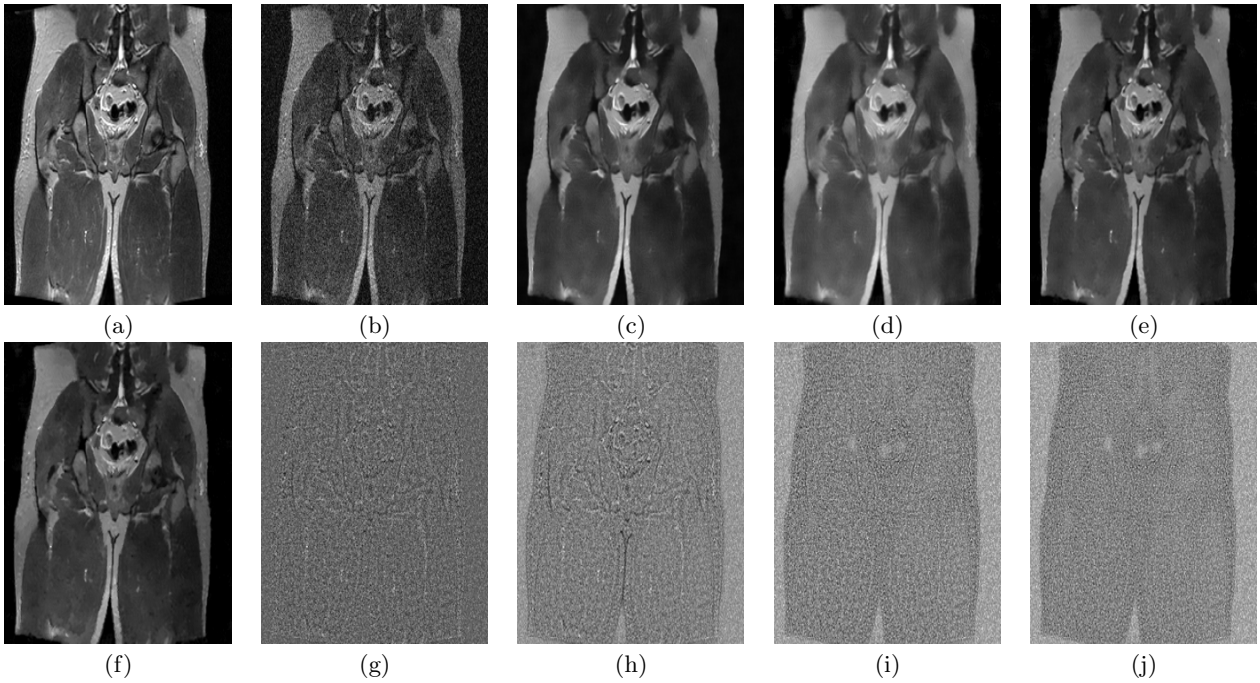

Figure 4: Real MR image : (a) Noise-free image, (b) noisy image (Rician noise level = 10%), (c) NLM-output [2], (d) UNLM-output [17], (e) IUNLM-output, (f) PCNN-AIUNLM output, (g) residual of NLM, (h) residual of UNLM, (i) residual of IUNLM and (j) residual of PCNN-AIUNLM.

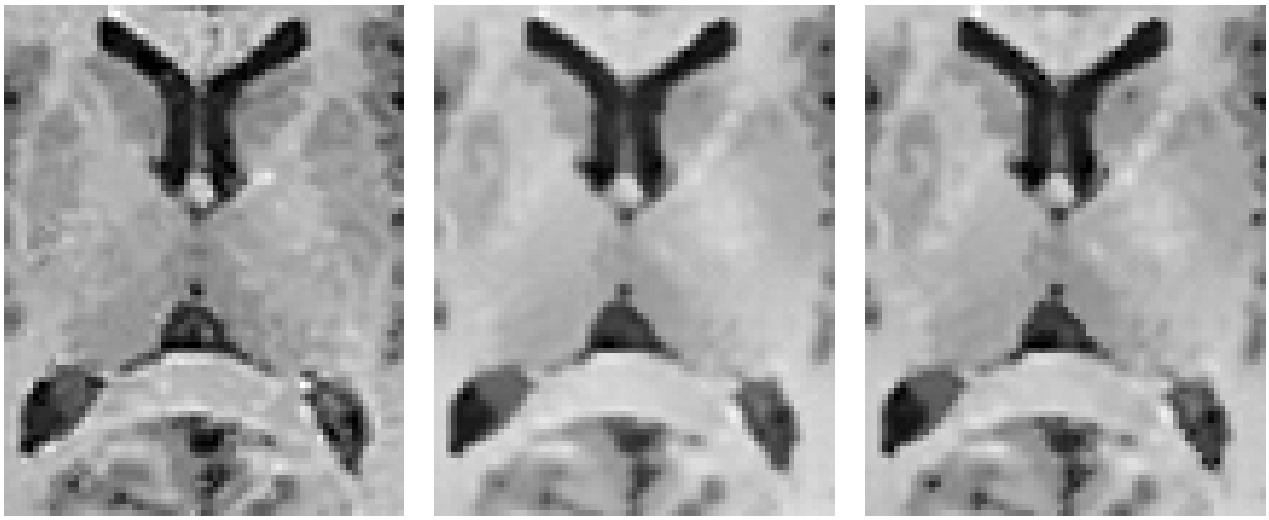

(a) (b) (c)

Figure 5: Zoomed in portion of the Synthetic MR image: (a) noise free (b) IUNLM (c) PCNN-AIUNLM.

4. EXPERIMENTAL RESULTS AND COMPARISONS

We implemented the proposed technique in MATLAB, and experiments were carried out on a PC with 2.66 GHz CPU and 4 GB RAM. To evaluate and compare the proposed denoising scheme with state-of-the-art techniques, we did experiments on various $2D$ MR images (both synthetic and real). For visualization purposes, the magnitude of the MR image is shown. Parameters of the PCNN were set to $\alpha_L = 1$, $V_L = 1$, $\beta = 3.5$, $\alpha_T = 0.5$, $V_T = 20$, $N = 200$ and M was set to the reciprocal of square distance between two pixels (coefficients) in a window of size $k \times l = 7 \times 7$. The value of the denoising parameter t was set to 15. These parameter values were found to provide satisfactory results and were estimated experimentally. The values of the parameters required in NLM filtering were set as $R_{sim} = 2$, $R_{search} = 5$ and $h = 1.2\sigma$ (as mentioned in [17]). Each of the medical images were contaminated by adding several levels of Rician noise $[1\%, 3\%, 5\%, 7\%, 9\%, 11\%]$. In this regard, $x\%$ represents the standard deviation ($xb/100$) of the added zero-mean white Gaussian noise, where b is the value of the brightest tissue in the image. The quantitative measures used in the experiments and comparisons were: root mean squared error (RMSE), peak signal-to-noise ration (PSNR) and structural similarity index (SSIM) [24].

The proposed denoising scheme was compared with 3 state-of-the-art MRI denoising techniques. The compared methods are: the standard NLM implementation proposed by Buades et al. [3]. the unbiased version of the NLM (UNLM) proposed by Manjón et al. [17] and the improved version of UNLM through pixel pre-selection by local mean (IUNLM). In order to evaluate the performance of the proposed scheme for synthetic MR data, tests were carried out on the images of BrainWeb database [1]. Experiments were conducted on 2D slices of 3D image volumes. Fig. 3, shows the visual results for a 2D slice of a T1-weighted MR image volume ($181 \times 217 \times 181$ with $1mm^3$ resolution) obtained by the proposed (PCNN-AIUNLM) method as well as several state-of-the-art existing schemes. This figure also contains the residual images obtained by subtracting the denoised images (obtained from different denoising techniques) from the noisy images. As can be observed from the residual images of Fig. 3 that the schemes NLM [3] and UNLM [17] have removed more anatomical information from the MR image compared to IUNLM and PCNN-AIUNLM. The denoised images (Fig. 3(e),(f)) obtained through IUNLM and PCNN-AIUNLM look very similar and the corresponding residual images (Fig. 3(i),(j)) also show evidence of removal of less anatomical information from the MR image.

To apply the PCNN-AIUNLM to real[1] magnitude MR images the standard deviation of the complex Gaussian noise needs to be estimated. In the experiments the noise estimation was carried out by the method proposed by Rajan et al. [22]. Fig. 4 show the visual performance of the proposed scheme in case of real MR image. From the given results for real MR images, it can be easily observed that the denoised images obtained by the proposed scheme along with the method IUNLM are producing the superior results compared to the other techniques. This is evident from the residual images given in Fig. 4. It can be clearly seen form these residual images that the proposed scheme and the improved version of UNLM (i.e., IUNLM) are causing less anatomical information loss and smoothing effects.

Even though, the denoised images obtained by the proposed scheme (PCNN-AIUNLM) and the technique of IUNLM look very similar. But, on a more careful inspection of the obtained results of these techniques reveal that the proposed scheme is producing slightly superior results by preserving the inherent subtle textural and structural information a bit better over IUNLM. The images of the Fig. 5 demonstrate the visual quality improvement of PCNN-AIUNLM over IUNLM. The Fig. 5 contains the images of the zoomed in portions of the synthetic MR image. We can see that

[1]Downloaded from http://bigwww.epfl.ch/luisier/MRIdenoising/TestImages.zip

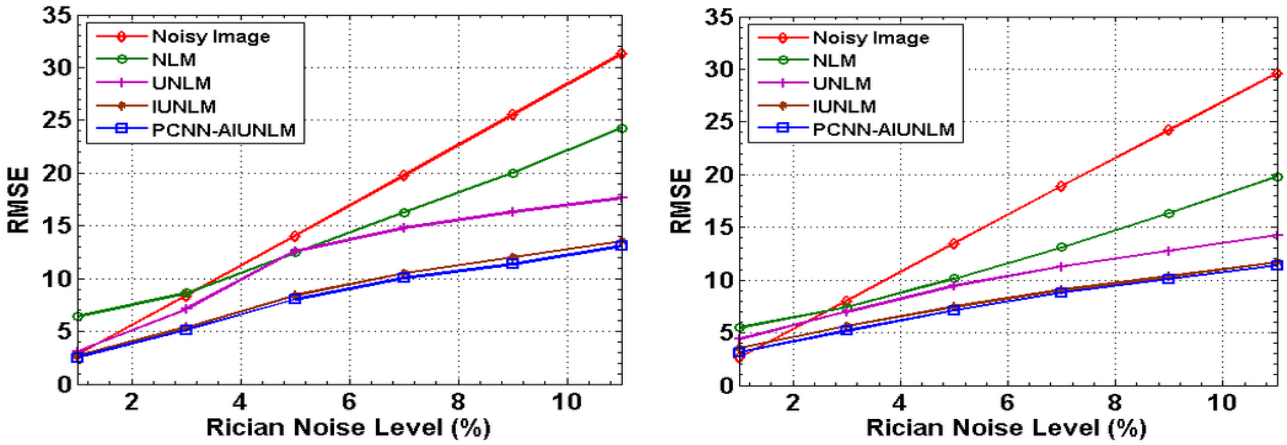

Figure 6: Performance comparison in terms of RMSE with different noise levels and image types: (a) synthetic MR image, (b) real MR image.

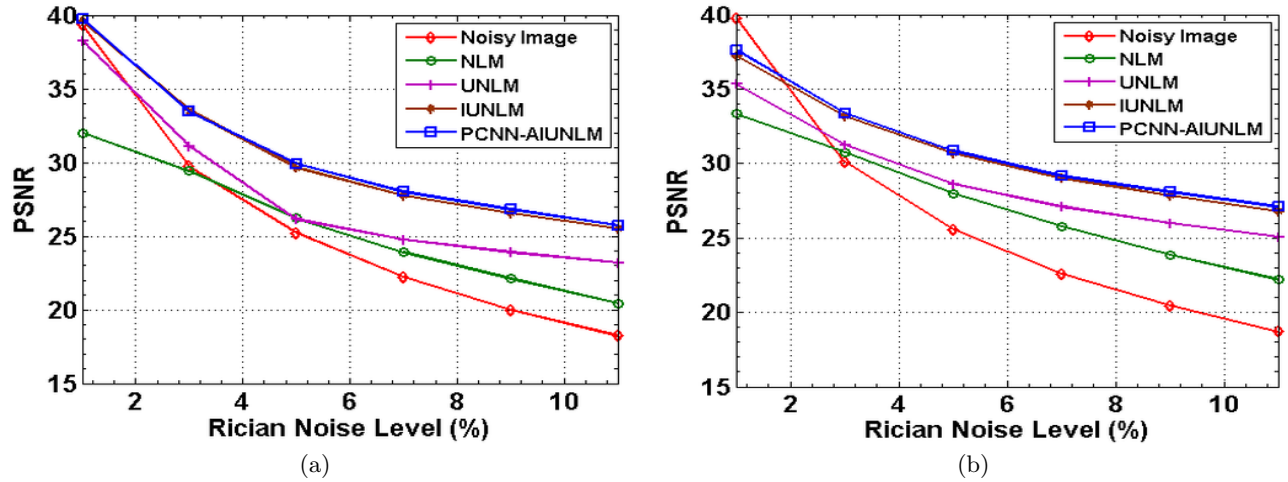

Figure 7: Performance comparison in terms of PSNR with different noise levels and image types: (a) synthetic MR image, (b) real MR image.

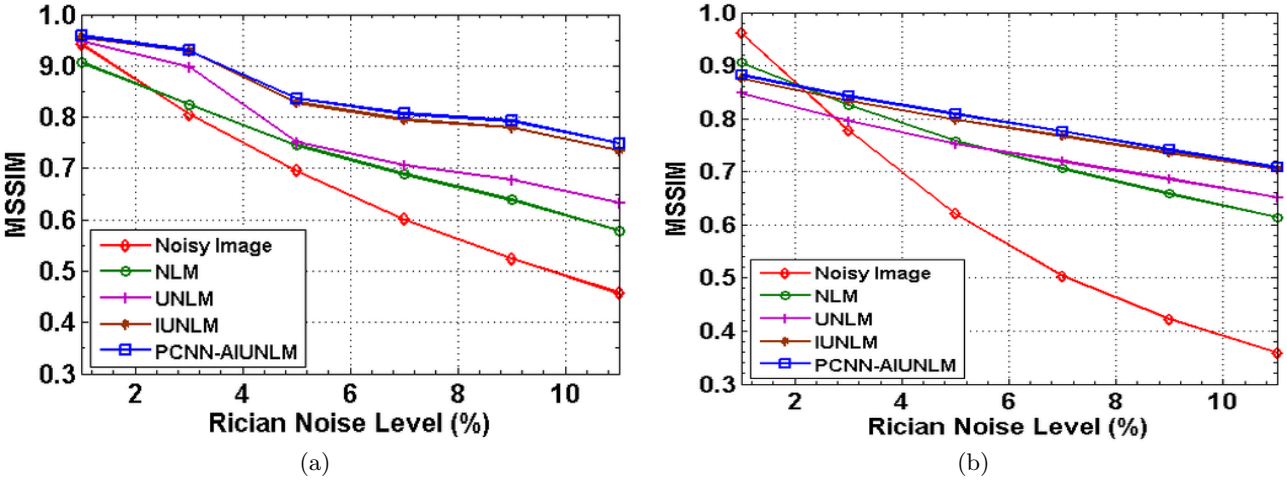

Figure 8: Performance comparison in terms of MSSIM with different noise levels and image types: (a) synthetic MR image, (b) real MR image.

Table 1: Performance comparison in terms of computation.

Image (Size)	Scheme	Measure	Noise Standard Deviation					
			1	3	5	7	9	11
Synthetic (181 × 217)	NLM	Iterations	2999940					
		Time (sec.)	14.5704					
	UNLM	Iterations	1499970					
		Time (sec.)	10.9668					
	IUNLM	Iteration	533333	689135	815668	929336	1010638	1119087
		Time (sec.)	4.0872	5.2104	6.0216	6.8640	7.6284	8.1432
	PCNN-AIUNLM	Iterations	**439994**	**580799**	**671653**	**754533**	**797551**	**859441**
		Time (sec.)	**3.9184**	**4.8828**	**5.4756**	**5.9904**	**6.6924**	**6.9732**
Real Image (256 × 256)	NLM	Iterations	7696260					
		Time (sec.)	39.1718					
	UNLM	Iterations	3848130					
		Time (sec.)	27.5029					
	IUNLM	Iterations	1748300	2217263	2564033	2792195	2964518	3099930
		Time (sec.)	14.5392	16.8481	19.3129	21.1537	22.4953	24.2113
	PCNN-AIUNLM	Iterations	**1420104**	**1809446**	**2103442**	**2281565**	**2391385**	**2485174**
		Time (sec.)	**12.4176**	**14.7888**	**17.2381**	**18.5641**	**19.4377**	**20.1553**

the scheme IUNLM results in slightly over-smoothing of the fine textural and structural details as compared to the proposed technique PCNN-AIUNLM. Due to the absence of this over-smoothing the denoised images obtained through PCNN-AIUNLM are visually better than the resultant images obtained by IUNLM.

The graphs of the Figs. 6-8, show the performance comparisons of the proposed scheme PCNN-AIUNLM with the techniques NLM, UNLM and IUNLM in terms of the quantitative measures RMSE, PSNR and MSSIM, respectively. These graphs show the effectiveness of the different denoising methods with increasing level of noise. In all the cases we have also included the corresponding quantitative measures for the noisy images (represented by the 'red' lines in the graphs). It is clear from the graphs of the Figs. 6-8 that IUNLM has superior performance over UNLM and NLM in all the cases. The proposed denoising scheme performs slightly better than IUNLM as indicated by the little differences between the graphs of PCNN-AIUNLM and IUNLM for the different quantitative measures of Figs. 6-8.

The real superiority of the PCNN-AIUNLM over the other compared methods comes in the form of computational efficiency. This is evident from the Table 1. This table contains the performance comparison of the proposed scheme over the before mentioned existing techniques in terms of total number of 'Iterations' and the actual 'Time (sec.)' requirements. The best measures in the Table 1 are denoted by 'bold' values. It is clear from the Table 1 that for all the MR images used in the experiments that PCNN-AIUNLM is the least computationally expensive scheme as compared to NLM, UNLM and IUNLM. We can see from the Table 1 that the denoising methods NLM and UNLM require the same number of iterations and time irrespective of the noise amount. But, for IUNLM and PCNN-AIUNLM the time requirements (total number of iterations and time in seconds) increase with increase in the noise amount. The obtained results and comparisons with state-of-the-art techniques suggest that the proposed scheme is effective in MRI denoising. The proposed method not only provides better denoised results, but also is less computationally expensive. Moreover, as both the NLM and the PCNN is highly parallelizable the processing time associated with this proposed scheme can be further reduced using distributed computing and more advanced version of the NLM filter.

5. CONCLUSION

Even though, there exists several MR image denoising methods based on the NLM paradigm. But, most of these schemes concentrate on either improving the denoising quality or reducing the computational burden. In this article we have proposed a novel and alternate way to pre-select a subset of pixels in the non-local vicinities of NLM paradigm, depending on their similarities with the pixel of interest. In the second step, improved version of UNLM is applied to denoise the pixel of interest only considering the contributions of the pre-selected subset of pixels in the non-local vicinities. The pre-selection of pixels is achieved by the time-signature of the noisy image obtained through PCNN. Experimental results and comparisons show that the proposed technique can simultaneously provides improved denoised MR images with lower computational cost. The proposed scheme can be incorporated with more improved version of the NLM filter to get superior results. Also, the extension of the proposed technique for 3D MR images should be carried out in future.

6. ACKNOWLEDGEMENTS

The authors would like to thank BrainWeb and F. Luisier (School of Engineering and Applied Sciences, Harvard University, Cambridge) for providing us with the MR images used in the experiments. This work is mainly funded by Machine Intelligence Unit, Indian Statistical Institute, Kolkata-108 (Internal Academic Project) for providing facilities to carry out this work. The authors also acknowledge Tata Consultancy Services for funding the registration fee of the conference. Malay K. Kundu acknowledges the Indian National Academy of Engineering (INAE) for their support through INAE Distinguished Professor fellowship.

7. REFERENCES

[1] http://www.bic.mni.mcgill.ca/brainweb/.

[2] A. Buades, B. Coll, and J. M. Morel. A non local algorithm for image denoising. In *Proc. Int. Conf. IEEE CVPR*, pages 60–65, 2005.

[3] A. Buades, B. Coll, and J. M. Morel. A review of image denoising algorithms with a new one. *Multiscale Modelling and Simulation*, 4(2):490–530, 2005.

[4] M. M. I. Chacon and A. Zimmerman. Image processing using the PCNN time matrix as a selective filter. In *Proc. of International Conference on Image Processing*, volume 1, pages 877–880, 2003.

[5] P. Coupe, J. V. Manjon, M. Robles, and D. L. Collins. Adaptive multiresolution non-local means filter for 3D MR image denoising. *IET Image Processing*, 6(5):558–568, 2012.

[6] P. Coupe, P. Yger, S. Prima, P. Hellier, C. Kervrann, and C. Barillot. An optimized blockwise nonlocal means denoising filter for 3-D magnetic resonance images. *IEEE Trans Med Img*, 27(4):425–441, 2008.

[7] S. Das and M. K. Kundu. NSCT-based multimodal medical image fusion using pulse-coupled neural network and modified spatial frequency. *Medical & Biological Engineering & Computing*, 50(10):1105–1114, 2012.

[8] S. Das and M. K. Kundu. A neuro-fuzzy approach for medical image fusion. *IEEE Transactions on Biomedical Engineering*, 60(12):3347–3353, 2013.

[9] R. Eckhorn, H. J. Reitboeck, M. Arndt, and P. Dicke. Feature linking via synchronization among distributed assemblies: Simulations of results from cat visual cortex. *Neural Computation*, 2(3):293–307, 1990.

[10] Y. Gal, A. J. H. Mehnert, A. P. Bradley, K. McMahon, D. Kennedy, and S. Crozier. Denoising of dynamic contrast-enhanced MR images using dynamic nonlocal means. *IEEE Trans. Medical Imaging*, 29:302–310, 2009.

[11] G. Gerig, O. Kubler, R. Kikinis, and F. A. Jolesz. Nonlinear anisotropic filtering of MRI data. *IEEE Trans Med Img*, 11(2):221–232, 1992.

[12] L. Ji and Z. Yi. A mixed noise image filtering method using weighted-linking PCNNs. *Neurocomputing*, 71:2986–3000, 2008.

[13] H. Liu, C. Yang, N. Pan, E. Song, and R. Green. Denoising 3D MR images by the enhanced non-local means filter for rician noise. *Magn. Reson. Imaging*, 28:1485–1496, 2010.

[14] Q. Liu and Y. Ma. A new algorithm for noise reducing of image based on PCNN time matrix. *Journal of Electronics & Information Technology*, 30(8):1869–1873, 2008.

[15] M. Lysaker, A. Lundervold, and X. C. Tai. Noise removal using fourth-order partial differential equation with applications to medical magnetic resonance images in space and time. *IEEE Trans Img Proc*, 12(12):1579–1590, 2003.

[16] Y. Ma, F. Shi, and L. Li. Gaussian noise filter based on PCNN. In *Proc. of International Conference on Neural Networks and Signal Processing*, volume 1, pages 149–151, 2003.

[17] J. V. Manjon, J. Carbonell-Caballero, J. J. Lull, G. G. Marti, L. Marti-Bonmati, and M. Robles. MRI denoising using non-local means. *Medical Image Analysis*, 12:514–523, 2008.

[18] J. V. Manjon, P. Coupe, L. Marti-Bonmati, D. L. Collins, and M. Robles. Adaptive nonlocal means denoising of MR images with spatially varying noise levels. *Journal of Magnetic Resonance Imaging*, 31:192–203, 2010.

[19] J. Mohan, V. Krishnaveni, and Y. Guo. A survey on the magnetic resonance image denoising methods. *Biomedical Signal Processing and Control*, 9:56–69, 2014.

[20] R. D. Nowak. Wavelet-based rician noise removal for magnetic resonance imaging. *IEEE Trans Img Proc*, 8(10):1408–1419, 1999.

[21] A. Pizurica, W. Philips, I. Lemahieu, and M. Acheroy. A versatile wavelet domain noise filtration technique for medical imaging. *IEEE Trans Med Img*, 22(3):323–331, 2003.

[22] J. Rajan, D. Poot, J. Juntu, and J. Sijbers. Noise measurement from magnitude MRI using local estimates of variance and skewness. *Physics in Medicine and Biology*, 55(16):441–449, 2010.

[23] A. Tristan-Vega, V. Garcia-Perez, S. Aja-Fernandez, and C. F. Westin. Efficient and robust nonlocal means denoising of MR data based on salient features matching. *Computer methods and programs in biomedicine*, 105(2):131–144, 2012.

[24] Z. Wang, A. C. Bovik, H. R. Sheikh, and E. P. Simoncelli. Image quality assessment: from error visibility to structural similarity. *IEEE Transactions on Image Processing*, 13:600–612, 2004.

[25] Z. Wang, Y. Ma, F. Cheng, and L. Yang. Review of pulse-coupled neural networks. *Image Vision and Computing*, 28(1):5–13, 2010.

[26] C. Westbrook. *Handbook of MRI Technique*. Wiley-Blackwell, USA, third edition, 2008.

[27] H. Zhang, Z. Zhang, L. Dong-mei, and Y. Ma. A novel image de-noising algorithm combined PCNN with morphology. In *Proc. of the 2007 International Conference on Neural Networks and Signal Processing*, pages 208–211, 2007.

[28] J. Zhang and M. S. J. Dong. An adaptive method for image filtering with pulsecoupled neural networks. In *Proc. of International Conference on Image Processing*, volume 2, pages 133–136, 2005.